IJME

Int. J. of Applied Mechanics and Engineering, 2024, vol.29, No.4, pp.24-32
DOI: 10.59441/ijame/192271

IMPROVEMENT FRICTION WELDED 6063 – T6 ALUMINUM ALLOY JOINT PROPERTIES

Basim M. A. Al Bhadle
Engineering Technical College - Baghdad, Middle Technical University, Baghdad, IRAQ

Safaa M. Hassoni * and Kharia Salman Hassan
Institute of Technology - Baghdad, Middle Technical University, Baghdad, IRAQ
E-mail: dr.safaa1970@mtu.edu.iq

This study aims to investigate the effect of shot peening on the mechanical characteristics and microstructure of an aluminum alloy 6063 friction welded joints. 6063 bars with *12 mm* diameters and *70 mm* lengths were prepared; some of them were shot peened by steel balls (diameters *1.25 mm*) for *15* minutes before the friction welding was carried out on a traditional lathe machine at *1200 rpm*. X-ray radiography was used to identify the various internal defects like porosity, concavities, and cracks. The quality of each welded joint was evaluated by hardness test, microstructure analysis, X-ray diffraction, tensile test, and bending test. It was discovered that the fine grain structure of the aluminum alloy weld connection matrix results in a strong and reliable shot peening, contributing to improving the tensile and bending strength of weld joints with a percentage of *63.6%* and *12.5 %*, respectively.

Key words: friction welding process; aluminum alloys; shot peen; mechanical properties.

1. Introduction

Heat-treatable alloy has good mechanical characteristics and contains *0.7%* magnesium and *0.4%* silicon commonly used as an architectural alloy. It is normally used in intricate extrusions. When the same materials are joined, the joint contact is successful, and the weld integrity is strong [1, 2]. American Welding Society (AWS) has classified friction welding as one of the solid-state joining methods and divided its techniques into friction stir welding (FSW) and friction rotary welding (FRW). FRW is the best welding method to join aluminum bars [3-5] because it produces a high joint strength with low distortion and flaws. Figure 1 shows the enough frictional heating is generated during FRW by the contact under the primary axial load between the rotating part and stationary part, and then the find axial force is applied to reason plastic movement and connection [6-8]. The heating is generated as a result of friction interaction between the fixing and spinning part [9, 10] to convert the mechanical energy into thermal energy, which is the fundamental idea behind the friction welding method. The bonding interface's temperature rises quickly, allowing the mass to flow and flex plastically in response to centrifugal force and applied pressure, producing a flash [11-13]. This method helps to create a surface with great chemical and physical adhesion by removing contaminants and oxides from the surface. Increased temperature and continuous pressure applied to the bonding interface for a predetermined amount of time allow the major constituents of the two materials to diffuse atomically, leading to their union. Shot peening is a cold working process; spherical balls are shot against a sample surface at velocities ranging from *20* to *100 m/s* during the cold working process known as shot peening. In order to create a layer of compressive residual stress at the surface of components exposed to fatigue or Stress corrosion failure, shot peening is frequently utilized. The characteristics of the material being shot peened and the particular peening parameters utilized determine the stress distribution that is created throughout the [14-17].

The only reliable way to control and optimize shot peening is to measure the residual stress distributions that are created below the surface [18, 19]. Mechanical property data such as tensile strength,

* To whom correspondence should be addressed

Hardness, and bending strength from tests have been performed. The weld and parent metal's micro structural features have been studied.

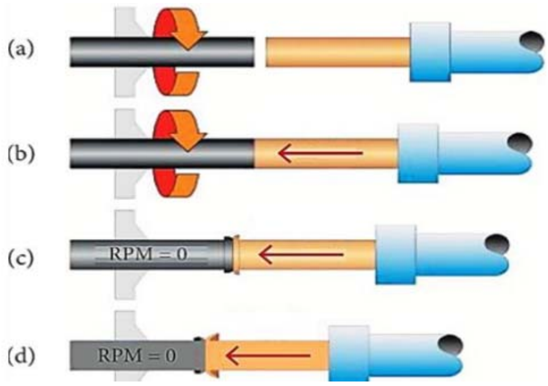

Fig.1. The principle of operation for the RFW process [6].

2. Experimental procedure

2.1. Metal select

The material used in this study is an aluminum alloy AA 6063-T6 (Fig.2), which was used in Architectural applications, Extrusions, window frames, Doors, and shop fittings, prepared into the required dimension (*70* lengths ×*12* diameter *mm*) by a lath machine. The faces of the original materials were prepared using *400* and *800* grit emery sheets previous to friction welding, and Tab.1 shows the chemical analysis by using an ARL Spectrometer; Tab.2 shows the mechanical properties of the alloy.

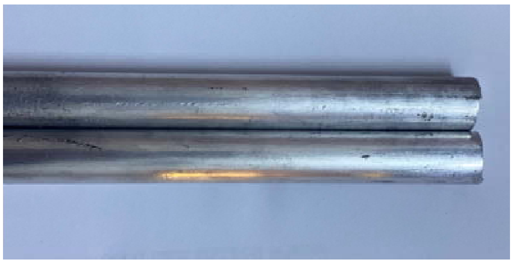

Fig.2. Aluminum 6063-T6 bars.

Table 1. Chemical analysis of 6063-T6 aluminum alloys.

Element (wt.)%	**Zn**	**Si**	**Mn**	**Mg**	**Fe**	**Cu**	**Cr**	**Ti**	**Al**
Actual	*0.2*	*0.45*	*0.25*	*0. 9*	*0.18*	*0.17*	*0.08*	*0.01*	Ram
Specification [20]	*0.25*	*0.4-0.8*	*0.15-0.4*	*0.8-1.2*	*0.7*	*0.15-0.4*	*0.04-0.35*	*0.15*	Ram

Table 2. Mechanical properties of AA6061-T6 aluminum alloy.

	Tensile strength N/mm^2	**Yield strength** N/mm^2	**Elongation** *%*
Specification [20]	*310*	*275*	*12*
Actual	*300*	*270*	*11*

2.2. Shot peening process

The shot peening method, which includes utilizing a steel ball with a *1.25 mm* diameter to significantly plastic formation on the specimen's surface for *15* minutes from all sides, was used to prepare shot peening samples. Using an air-blast machine tumbles control model (STB – OB) machine No. 03008 05, the nozzle askew is inclined by $10°$ with respect to the perpendicular axis. The specimen Fig.3 was spaced *120 mm* apart from the nozzle and shot at a speed of *40 m/min*. The strain resulting from shot peeing in the crystal lattice and the amount used in brag law to account for the compressive residual stress in the shot peening material were measured using a computerized device (Lab XRD-6000 Shiatsu X-RAY diffraction meter). The residual stress results from the device were $(-143MPa)$.

Fig.3. Shot peening machine with shot balls.

2.3. Surface roughness

The surface roughness of the base material (USP) sample was measured using a pertho metre type (S6P) at the surface area of the base alloy and shot peened specimens. The parameter *Ra*, which is the center-line average of adjacent samples, indicated the average surface roughness of these samples. The average surface roughness of the shot-peened samples was *2*, *1* μm.

2.4. Friction welding

Friction welding is carried out using a conventional lathe machine, as shown in Fig.4. Based on earlier studies, the welding is done at a speed of *1200 rpm* and *8* bar forge pressure. A female component of the face geometry is present on the initial piece of 6063-T6 alloy, which is connected to the chuck during the welding process. The second piece, on the other hand, is attached to the lathe machine's tailstock and features a male face geometry part.

The spindle will move downward to apply the predetermined axial force once the desired rate is reached. These conditions were validated for an extended duration. The load is applied in the following phase until the required temperatures $(520°C)$ and material state are maintained. At this point in the procedure, the materials undergo plasticization as soon as the element reaches the appropriate span. The rotating speed is stopped. Following that, the axial force starts to work to provide "forge pressure" to complete the weld. This provides grain refining and molecular bonding during the welding process.

Fig.4. Lathe machine.

2.5. X-ray radiography testing

To examine the several internal flaws, such as porosity, concavities, cracks, cold laps, slag, etc., X-ray radiography was used. Using X-ray radiography, all samples of aluminum alloy 6063-T6 manufactured by friction welding were inspected to look for any flaws, primarily at the weld junction. Every sample showed no indication of a flaw or discontinuity. Because no melting occurs during the welding process and the heat produced by the friction between the workpieces joins the metals in a solid state, friction-welded connections are free from flaws associated with solidification.

2.6. X-ray diffraction

By employing SHIMADZU-6000XRD for X-ray diffraction analysis, the phases of the specimens were determined. Cu $(=1.54060\,A^{\circ})$ target, *30 mA* current, *40 kV* voltage, and a *10-90* degree scan range were the parameters under which this was carried out. The findings are displayed in Fig.5.

2.7. Microstructural test

Samples were examined under an optical microscope after being prepared for microstructures in the following steps: grinding, polishing, and etching. Emery paper made of SiC with varying grits (*240*, *400*, *600*, and *1000*) was used for the wet grinding process with water. The samples were polished using a special polishing cloth and diamond paste with a size of *1 µm*. After being cleaned with alcohol and water, they were dried with hot air. Samples were etched using Keller's reagent (etching solution), which included *2 ml* HF, *3 ml* HCl, *5 ml* HNO_3, and *190 ml* water [21]. The samples were then rinsed with water and alcohol and dried. A Nikon ME-600 optical microscope, along with an NIKON camera, was used to evaluate the microstructures.

2.8. Rockwell B hardness test

To evaluate the mechanical qualities of welding joints, the Rockwell B hardness test was utilized. The hardness was measured at the plane perpendicular to the longitudinal axis. Three different measurements are taken at different randomly selected sites to estimate the average hardness. The results are listed in Tab.3.

Table 3. Hardness Rockwell B result.

Symbol of specimens	As received	As welded	Shot peen+ welded
Rockwell B hardness Kg/mm^2	*80*	*55*	*70*

2.9. Tensile stress and bending test

Many specimens for the tensile test are manufactured from weld and 6063-T6 according to ASTM E 8M, to test using Testing machine smart series crosshead speed $(1\,mm/min)$.

At room temperature, exterior face bending investigations are performed using the three-point method. The central line of the specimen receives a line load in the shape of a cylinder. At a speed of $3.5\,mm/min$, this test was conducted on a $100\,kN$ universal to determine the specimens' strength.

3. Results and discussion

X-ray radiography is used at the weld joint in order to detect any flaws. All samples were free of defects. The XRD results of Al 6063-T6 alloy are shown in Fig.5. The intensity peak corresponding to the Mg_2Si precipitate is observed. Due to the presence of alloying elements such as silicon and magnesium, which provide strong mechanical properties, the microstructure, as shown in Fig.6, shows the coarse Mg_2Si precipitate phase (Figs 6c and 6e) with the fine aluminum matrix in the plastic deformation layers (Figs 6a, 6b and 6C) causes inhomogeneity welding joint (Figs 6a and 6d). While shot peening with friction force are produced the fine equiaxed Mg_2Si grain size (Figs 7a, 7b, 7d, and 7e) by crushing coarse grains in the base metal (Fig.7c).

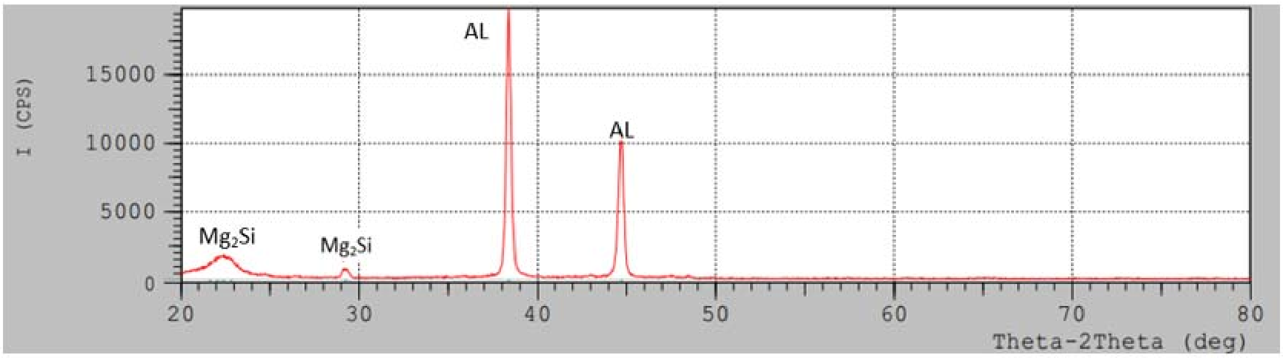

Fig.5. The X-Ray Diffraction Result for 6063-T6.

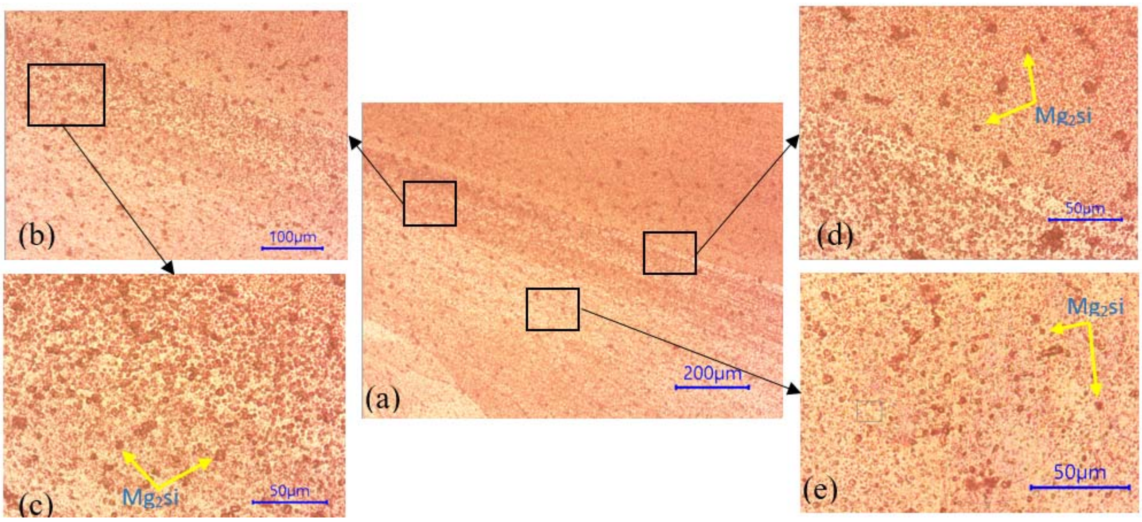

Fig.6. Show the microstructure of welding joint without shot peen.

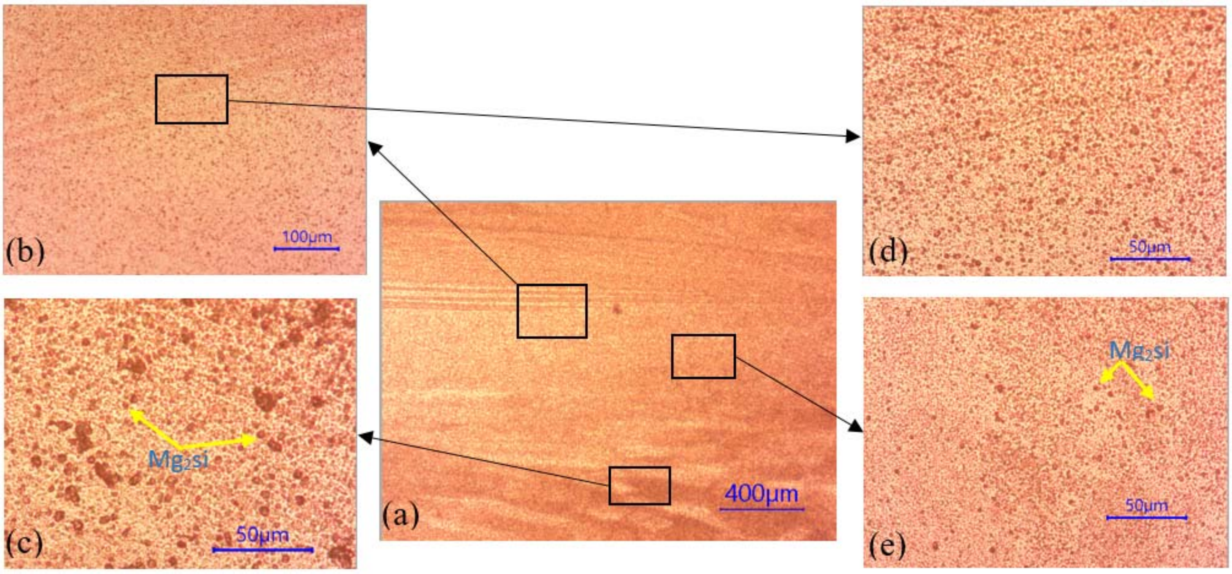

Fig.7. Show the microstructure of the welding joint after shot peen.

The tested results are listed in Tab.4 and Fig.8. The absence of melting during the welding process and the heat produced by the friction between the workpieces ensure that friction-welded joints are free from welding defects. The strength of the weld region is lower than that of the original parent and bend test. Welding specimens without a shot has a very low bend angle without any cracks from the weld zone, the results are shown in Tab.5 and Fig.9. In other words, the bending stress is lower when it compared with base metal because of the crack began at a small bending angle. Tensile and bending test results with using the shot peening increase a slightly than without a shot. So, shot peening was contributed to improve the tensile and bending strength. It was seen that the aluminum alloy matrix shows fine grain structure compressive residual stress.

(a)Tensile Test device

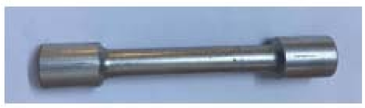

(b) Tensile test specimens

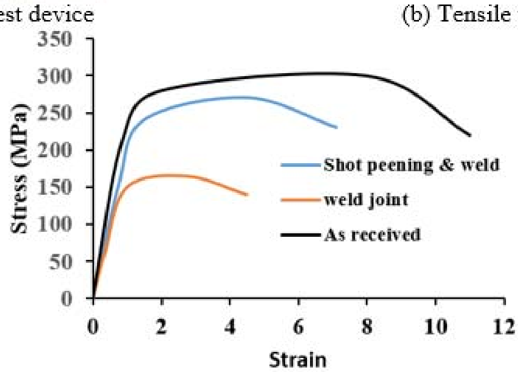

(c) Tensile test result for all specimens.

Fig.8. (a) tensile device, (b) tensile test specimen (c) tensile test result.

Table 4. Tensile test results for all specimens.

Specimens	$\sigma y\ MPa$	$\sigma U\ MPa$	$\sigma F\ MPa$	ϵ
As received	*270*	*300*	*220*	*11*
Weld joint	*150*	*165*	*140*	*4.5*
Shot peen+ welding	*230*	*270*	*220*	*6*

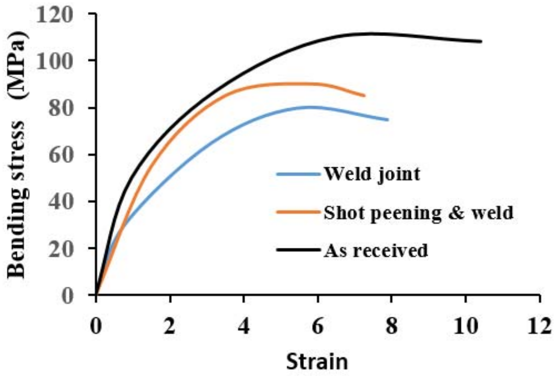

Fig.9. Bending test result for all specimens.

Table 5. Bending test results for all specimens.

Specimens	$\sigma U\ MPa$	$\sigma F\ MPa$	ϵ
As Received	*110*	*108*	*10.4*
As welding	*80*	*75*	*7.8*
Shot peen &welding	*90*	*85*	*7.25*

4. Conclusion

1. All samples passed the x-ray radiography test without any defects or discontinuities, indicating that friction welding, when done correctly, has a very low possibility of producing weld joint defects.
2. The Microstructure of shot peen samples was refined.
3. Shot peening created a compressive film that increased the tensile and bending strengths by *63.6%* and *12.5 %* percent, respectively.
4. Hardness increases as a result of strain hardening following shot peening.

Acknowledgments

We want to thank the Department of Technical Applied Mechanical Engineering, Engineering Technical College - Baghdad, Middle Technical University, Baghdad, Iraq.

Nomenclature

AWS – American Welding Society
FSW – friction stir welding
FRW – friction rotary welding
AA – aluminum alloy
HF – hydrofluoric acid

HCl – hydrochloric acid
HNO_3 – nitric acid
ASTM – American Society for Testing and Materials
XRD – X-ray diffraction

References

[1] Dash P.K., Vishal G.R., Vinod L., Mahendra M.A. and Manvi P. (2021): *Characterization of strength of aluminum (Al 6063-T6) after corrosion.*– Journal of Experimental and Applied Mechanics, vol.12, No.3, pp.48-61, DOI: 10.37591/JoEAM.

[2] Muad Muhammed Ali, Haidar Akram Hussein, Nabil Kadhim Taieh, Ying Li, Riad Abdul Abas, Sumair Ahmed Soomro, and Salman Aatif (2024): *Enhancing the tribological characteristics of epoxy composites by the use of three-dimensional carbon fibers and cobalt oxide nanowires*.– Journal of Techniques, vol.6, No.2, pp.29-35, https://doi.org/10.51173/jt.v6i2.2439.

[3] Alves E.P., Toledo R.C., Piorino F., Botter F.G. and Ying An C. (2019): *Experimental thermal analysis in rotary friction welding of dissimilar materials*.– Journal of Aerospace Technology and Management, vol.11, e4019, https://doi.org/10.5028/jatm.v11.1068.

[4] Kareem Abbas Falih, Isam Jabbar Ibrahim, Sabah Khammass Hussein and Salah Mezlini. (2023): *Investigation of using the IL-FSSW technique to weld AA5052-H112 alloy with copper: experimental study*.– Journal of Techniques, vol.5, No.4, pp.105-114, https://doi.org/10.51173/jt.v5i4.1950.

[5] Hamzah M.M., Barrak O.S., Abdullah I.T., Hussein A.A., Hussein S.K. (2024). *Process parameters influence the mechanical properties and nugget diameter of AISI 316 stainless steel during resistance spot welding*.– International Journal of Applied Mechanics and Engineering, vol.29, No.2, pp.79-89, https://doi.org/10.59441/ijame/186956.

[6] Joshi S. (2022): *Investigation of rotary friction welded 6063-T6 and 6082-T6 aluminum alloy joint properties.*– International Journal of Mechanical Engineering. vol.7, No.3. pp.1-7.

[7] Alves E.P., Toledo R.C., Piorino F., Botter F.G., and Ying An C. (2019): *Experimental thermal analysis in rotary friction welding of dissimilar materials.*– Journal of Aerospace Technology and Management, vol.11, e4019, https://doi.org/10.5028/jatm.v11.1068.

[8] Barrak O.S., Hamzah M.M. and Hussein S.K. (2022): *Friction stir spot welding of pure copper (C11000) with pre-holed threaded aluminum alloys (AA5052)*.– Journal of Applied Science and Engineering, vol.26, No.8, pp.1103-1110, https://doi.org/10.6180/jase.202308_26(8).0006.

[9] Sakthivel T., Sengar G.S. and Mukhopadhyay J. (2009): *Effect of welding speed on microstructure and mechanical properties of friction-stir-welded aluminum.*– The International Journal of Advanced Manufacturing Technology, vol.43, No.5, pp.468-473, https://doi.org/10.1007/s00170-008-1727-7.

[10] Shen J.J., Liu H.J. and Cui F. (2010): *Effect of welding speed on microstructure and mechanical properties of friction stir welded copper*.– Materials and Design, vol.31, No.8, pp.3937-3942, https://doi.org/10.1016/j.matdes.2010.03.027.

[11] Barrak O.S., Sami Chatti and Slim Ben-Elechi. (2024): *Influence of welding parameters on mechanical properties and microstructure of similar low-carbon steel AISI 1005 welding by resistance spot welding*.– Journal of Techniques, vol.6, No.1, pp.45-51, https://doi.org/10.51173/jt.v6i1.2114.

[12] Rodrigues D.M., Loureiro A.L.C.L.R., Leitao C., Leal R.M., Chaparro B.M. and Vilaça P. (2009): *Influence of friction stir welding parameters on the microstructural and mechanical properties of AA 6016-T4 thin welds*.– Materials and Design, vol.30, No.6, pp.1913-1921, https://doi.org/10.1016/j.matdes.2008.09.016.

[13] Hassoni S.M., Barrak O.S., Ismail M.I. and Hussein S.K. (2022): *Effect of welding parameters of resistance spot welding on mechanical properties and corrosion resistance of 316L*.– Materials Research, vol.25, e20210117, https://doi.org/10.1590/1980-5373-MR-2021-0117.

[14] Prevéy P.S. (2000): *The effect of cold work on the thermal stability of residual compression in surface enhanced IN718*.– In Proceedings of the 20th ASM Materials Solutions Conference and Exposition, pp.10-12.

[15] Rawat M. and Singh R.N. (2022): *A study on the comparative review of cool roof thermal performance in various regions*.– Energy and Built Environment, vol.3, No.3, pp.327-347, https://doi.org/10.1016/j.enbenv.2021.03.001.

[16] Osamah Sabah Barrak, Mahmood Mohammed Hamzah, Ali Safaa Ali, Slim Ben-Elechi, Sami Chatti, Wasaq Haider Moubder, Ruba Rasool Radhi, Arfan Ali Ahmad. (2023): *Joining of polymer to aluminum alloy AA1050 by friction spot welding*.– Journal of Techniques, vol.5, No.4, pp.88-94, https://doi.org/10.51173/jt.v5i4.1976.

[17] Nie B., Palacios A., Zou B., Liu J., Zhang T. and Li Y. (2020): *Review on phase change materials for cold thermal energy storage applications*.– Renewable and Sustainable Energy Reviews, vol.134, p.110340, https://doi.org/10.1016/j.rser.2020.110340.

[18] Patil H.S., and Soman S.N. (2013): *Influence of weld process parameters on material characterization of friction stir welded joints of aluminium alloy AA6061-T6*.– International Journal of Advanced Design and Manufacturing Technology, vol.6, No.4(25), pp.9-15, https://sid.ir/paper/619051/en.

[19] Uday K.N. and Rajamurugan G. (2023): *Influence of process parameters and its effects on friction stir welding of dissimilar aluminium alloy and its composites-a review*.– Journal of Adhesion Science and Technology, vol.37, No.5, pp.767-800, https://doi.org/10.1080/01694243.2022.2053348.

[20] *Properties and Selection: Nonferrous Alloys and Special-Purpose Materials*.– ASM Handbook Volume 2, ASM International, OH, 1990.

[21] Ahuir Torres J. (2023): *Microscopy techniques to analyse the characteristics of the metallic materials*.– Journal of Materials and Electronic Devices, vol.1, No.1, pp.33-53.

Received: May 17, 2024
Revised: August 12, 2024